THE JOURNAL OF BIOLOGICAL CHEMISTRY
Vol. 276, No. 3, Issue of January 19, pp. 2139–2152, 2001
Printed in U.S.A.

Relationship between Novel Isoforms, Functionally Important Domains, and Subcellular Distribution of CD164/Endolyn*

Received for publication, August 31, 2000, and in revised form, October 6, 2000
Published, JBC Papers in Press, October 10, 2000, DOI 10.1074/jbc.M007965200

James Yi-Hsin Chan‡, Jane E. Lee-Prudhoe‡, Britt Jorgensen‡, Gudrun Ihrke§, Regis Doyonnas‡, Andrew C. W. Zannettino¶, Veronica J. Buckle‡, Christopher J. Ward‡, Paul J. Simmons‖, and Suzanne M. Watt‡

From the ‡Medical Research Council Molecular Hematology Unit, Institute of Molecular Medicine, Oxford OX3 9DS, United Kingdom, the §Wellcome Trust Centre for Molecular Mechanisms in Disease and the Department of Clinical Biochemistry, University of Cambridge, Cambridge CB2 2XY, United Kingdom, the ¶Hanson Centre for Cancer Research, Institute of Medical and Veterinary Sciences, Adelaide, 5000 South Australia, Australia, and the ‖Peter McCallum Cancer Institute, Melbourne, 3002 Victoria, Australia

Functional analyses have indicated that the human CD164 sialomucin may play a key role in hematopoiesis by facilitating the adhesion of human CD34$^+$ cells to the stroma and by negatively regulating CD34$^+$CD38$^{lo/-}$ cell proliferation. We have identified three novel human CD164 variants derived by alternative splicing of *bona fide* exons from a single genomic transcription unit. The predominant CD164(E1–6) isoform, encoded by six exons, is a type I transmembrane protein containing two extracellular mucin domains (I and II) interrupted by a cysteine-rich non-mucin domain. The 103B2/9E10 and 105A5 epitopes, which specify ligand binding characteristics, are located on the exon 1-encoded mucin domain I. Three human *CD164(E1–6)* mRNA species, exhibiting differential polyadenylation site usage, are differentially expressed in hematopoietic and non-hematopoietic tissues. This study provides additional evidence that human CD164(E1–6) represents the ortholog of murine MGC-24v and rat endolyn. Comparative analysis of murine MGC-24v/CD164(E1–6) with human CD164(E1–6) revealed two potential splice variants and a similar genomic structure. Whereas the human *CD164* gene is located on chromosome 6q21, the mouse gene occurs in a syntenic region on chromosome 10B1–B2. By confocal microscopy, human CD164 in CD34$^+$CD38$^+$ hematopoietic progenitor (KG1B) and epithelial cell lines appears to be localized primarily in endosomes and lysosomes, with low concentrations at the cell surface. However, in a minority of KG1B cells, CD164 is more prominently expressed at the plasma membrane and in the recycling endosomes, suggesting that its distribution is regulated in cells of hematopoietic origin.

The hematopoietic system is composed of a continuum of cells that are hierarchically ordered on the basis of their proliferative and differentiation potentials. At its apex is a rare population of slowly cycling pluripotent hematopoietic stem cells that are not only capable of extensive proliferation or commitment to one of nine lymphoid or myeloid cell lineages, but also have remarkable versatility with their ability to be reprogrammed into non-hematopoietic lineages (reviewed in Refs. 1 and 2). Hematopoietic stem cells and their progeny migrate to and colonize a series of hematopoietic sites during ontogeny. Under steady-state conditions, adult hematopoiesis is restricted mainly to the bone marrow, where hematopoietic and mesenchymal stem cells and their progeny reside in specific microenvironmental niches composed of phenotypically and functionally heterogeneous stromal cells and their associated biosynthetic products, including cytokines, chemokines, and adhesion ligands. Stem cell fate (*i.e.* migration, homing, cell positioning, differentiation, survival, proliferation, commitment, specific gene expression, reprogramming, and death or apoptosis) is regulated by external cues provided by the associated microenvironmental niche. Recent studies have implicated cooperative interactions between cytokine, chemokine, adhesion, and signaling receptors on hematopoietic stem cells and their progeny as key elements in detecting, translating, and fine-tuning these extrinsic cues (reviewed in Refs. 3 and 4). Despite this, the precise mechanisms of hematopoietic stem cell trafficking and localization within microenvironmental niches in adult and fetal development remain to be determined. The identification of the full complement of receptor/ligand interactions and the molecular mechanisms that determine their involvement in regulating stem cell fate therefore remains one of the major investigative areas in hematopoiesis.

We have recently identified and cloned human CD164, a novel 80–100-kDa sialomucin expressed, although not exclusively, by CD34$^+$ and CD34$^{lo/-}$ hematopoietic stem cells and associated microenvironmental cells (5–12). It contains, in its extracellular region, two mucin domains (I and II) linked by a non-mucin domain, which has been predicted to contain intradisulfide bridges (12). Functional analyses *in vitro* have indicated that this receptor may play a key role in hematopoiesis by facilitating the adhesion of human CD34$^+$ cells to bone marrow stroma and by negatively regulating CD34$^+$CD38$^{lo/-}$ hematopoietic progenitor cell proliferation (5). These effects involve the CD164 class I and/or II epitopes recognized by the monoclonal antibodies (mAbs)[1] 105A5 and 103B2/9E10 (9).

* This work was supported by the Leukaemia Research Fund, the Medical Research Council, an Overseas Research Student award, and the Wellcome Trust, United Kingdom. The costs of publication of this article were defrayed in part by the payment of page charges. This article must therefore be hereby marked "*advertisement*" in accordance with 18 U.S.C. Section 1734 solely to indicate this fact.

The nucleotide sequence(s) reported in this paper has been submitted to the GenBank™/EBI Data Bank with accession number(s) AF299340 (human genomic CD164), AF299341 (human CD164(E1–6) cDNA), AF299342 (human CD164(ΔE5)), AF299343 (human CD164(ΔE4)), AF299344 (mouse genomic CD164), and AF299345 (mouse CD164-(E1–6)).

** To whom correspondence should be addressed: MRC Molecular Hematology, Inst. of Molecular Medicine, John Radcliffe Hospital, Headington, Oxford OX3 9DS, United Kingdom. Tel.: 44-1865-222-632; Fax: 44-1865-222-500; E-mail: Swatt@molbiol.ox.ac.uk.

[1] The abbreviations used are: mAb, monoclonal antibody; GM-CSF,

These epitopes are carbohydrate-dependent and are located on the amino-terminal mucin domain I (6, 7, 9). Recently, Kurosawa *et al.* (13) and Ihrke *et al.* (12) demonstrated that murine MGC-24v and rat endolyn share significant sequence similarities with human CD164 (5).

Our aim in this work was to define the size, diversity, and subcellular distribution of the human CD164 family and to compare the structural organization and chromosomal location of the human *CD164* gene with its murine counterpart as a first step toward more precisely exploring the functional role of this molecule *in vivo* in murine model systems and *in vitro*. Toward this end, we surveyed both human and murine RNAs from many different normal tissues and transformed cell lines for alternatively spliced isoforms. We have further defined the complete genomic structure of these human and murine genes and show that they possess similar genomic structures and similar chromosomal localizations. These results place CD164 within the mucin subgroup that is composed of multiple exons and further demonstrate the diverse chromosomal distribution of this family of molecules. Structural features and subcellular localization studies support the view that murine MGC-24v and rat endolyn genes are the orthologs of human CD164. The new CD164(E1–6) isoform, the major translated product, most closely resembles the described murine and rat cDNAs. The finding of additional novel variants of human CD164 extends the repertoire of the CD164 transmembrane receptor isoforms to four members and suggests that these may differentially interact with cognate ligands to modulate the activity of CD164 *in vivo* on a variety of cellular targets.

EXPERIMENTAL PROCEDURES

Cell Cultures—The cell lines TF1, KG1A, KG1B, U937, K562, Calu-1, A431, and KATO-III were maintained in RPMI 1640 medium containing 10% (v/v) fetal calf serum. TF1 also required 2 μg/ml recombinant human GM-CSF (R&D Systems, Abingdon, United Kingdom) for growth. Human bone marrow was collected with informed consent and appropriate ethical approval. Human bone marrow stromal reticular cells and $CD34^+$ progenitor subsets were isolated and cultured as described previously (5).

Inhibition of Cell Growth—The effects of engagement of the CD164 molecule by the CD164 class II mAb 103B2/9E10 on recruitment of cells into the cell cycle were determined in single cell assays as described previously (5). To measure the effects of the CD164 mAbs on nucleated cell production, $CD34^+$ cells (10^3 cells/culture) were cultured in triplicate in serum-deprived medium containing 10 ng/ml each purified recombinant IL-1β, IL-3, IL-6, G-CSF, GM-CSF, and Steel factor with 10 μg/ml mAb 103B2/9E10, 105A5, mIgG3, or mIgM. Additional cytokines and mAbs were added on days 7, 14, and 21, and nucleated cells were counted at weekly intervals. To examine the effect of engagement of the CD164 molecule on the growth and development of committed hematopoietic progenitor cells, 561-Dynabead (Dynal, Oslo, Norway)-purified $CD34^+$ cells (10^3) were incubated with either purified mAb 103B2/9E10 or 105A5 or isotype-matched mIgG3 or mIgM control mAb at concentrations ranging from 0.01 to 30 μg/ml for 1 h at 4 °C. Cells were plated in 0.9% (w/v) methylcellulose (Dow Chemicals, Lake Jackson, TX) supplemented with a 10 ng/ml concentration of each of the recombinant human cytokines IL-1β, IL-3, IL-6, G-CSF, GM-CSF, Steel factor, and erythropoietin (5). Erythroid burst-forming units (BFU-E) and granulocyte/macrophage colony-forming cells (GM-CFC) were counted at day 14 of culture (5).

CD164 cDNA Probes—Screening of the human PAC library and subclones and the probing of Southern blots were carried out with the human *CD164* cDNA probes h1, h2, h3, and h4, derived from the 105A5 cDNA clone (5, 6) (see the legend to Fig. 1) in the pGEM T vector (Promega, Madison, WI). The murine *CD164* cDNA was prepared by PCR amplification of BALB/c mouse heart first strand cDNA (CLONTECH, Palo Alto, CA) using primers mF164 and mCD164-SR or mR164 (see Table I) to the murine *MGC-24* cDNA sequence (13) in the DDBJ/GenBank™/EBI Data Bank (accession number AB028895). Screening of the murine PAC library and subclones and Southern blotting were carried out with the murine *CD164* cDNA probes m1 and m2 (described in the legend to Fig. 6*A*). Each cDNA probe (20–50 ng) was labeled with 50 μCi of [α-^{32}P]dCTP (Amersham Pharmacia Biotech, Buckinghamshire, UK) using the T7 Quickprime or Megaprime kit (Amersham Pharmacia Biotech, Uppsala, Sweden) as described previously (6).

Southern Blots of Genomic DNA—A Southern blot containing human placental DNA digested with *Eco*RI, *Hin*dIII, *Bam*HI, *Pst*I, and *Bgl*II was obtained from CLONTECH. Mouse strain 129 genomic DNA (15 μg/digest) was similarly digested and Southern-blotted onto Zeta-Probe membrane (Bio-Rad, Hertfordshire, UK) as described (6). These blots were hybridized with α-^{32}P-labeled human *CD164* probe h3 or murine probe m1.

Isolation and Subcloning of PAC Clones—The human PAC library derived from normal human male genomic DNA and the murine PAC (RPC121) library derived from 129/Svev TACfBr mouse spleen genomic DNA in the pCYPAC2N and pPAC4 vectors, respectively, and gridded onto Hybond N filters were provided by the Human Genome Mapping Project Resource Centre (Cambridge, UK). These filters were probed with α-^{32}P-labeled human h1 and h2 and murine m1 and m2 CD164 probes as described above. One positive PAC clone containing human *CD164* was selected and digested with *Bam*HI into three fragments (B3, B2, and B1 fragments), and the B1 fragment was divided by the *Bgl*II restriction site into four fragments (Bgl3.25, Bgl2.61, Bgl7.1, and Bgl4 fragments) and then subcloned into similarly digested pCRScript(SK+) vectors (see Fig. 1). The *CD164* gene inserts were sequenced directly using oligonucleotide primers derived from the cDNA and genomic DNA. Alternatively, using pCRScript SK(+) vectors containing the B2 and B3 inserts and the Bgl2.61, Bgl3.25, Bgl4, and Bgl7.1 inserts as templates, nested deletions were generated using the Erase-a-Base technique and the Erase-a-Base® kit (Promega) according to the manufacturer's instructions prior to automatic sequencing using M13 forward or reverse primers. To confirm the junctions between the *Bam*HI and *Bgl*II fragments, PCRs on the human PAC clones were carried out using the Expand Long Template system (Roche Molecular Biochemicals, Mannheim, Germany) and the following primer pairs: B3-PCR-F1 and B2-PCR-B1, CD164–2KF2 and MGC-GP-B1, B3.5-R2 and B2.5-F6, B2.5-RF7 and B7-R3, and B7-F2 and B4-FR3 (see Table I). The PCR products were polyethylene glycol-precipitated and sequenced directly using the same primers (6). One mouse PAC clone was selected, digested with *Bam*HI or *Eco*RI, subcloned into similarly digested pCRScript(SK+) vectors, and PCR-amplified using M13 forward and reverse primers or primers to the cDNA, and the PCR products were sequenced (6).

These sequences and those described below were analyzed using MacVector, Seqed, Assemblign, Analysis, and Sequencher software packages and aligned with each other and with the *CD164* cDNAs, and a contig was generated. Sequence data were then analyzed by accessing MacVector and the Prosite (Swiss Institute of Bioinformatics (SIB)), GenBank™, EMBL, and NCBI Databases for alignment, homology, *N*-glycan, hydropathy, and motif analyses. O-glycbase on the NCBI site was used for predicting *O*-glycosylation sites. The signal, transmembrane, and polyadenylation sites were predicted using Signal P (14), TMHMM (15), and WebGene HC-PolyA (16) programs, respectively.

Chromosomal Localization of the Murine CD164 Gene—Fluorescence *in situ* hybridization analysis was carried out essentially as described by Buckle and Rack (17). Murine digoxigenin-labeled PAC was co-hybridized with a commercial biotin-labeled mouse chromosome 10 paint (Cambio, Cambridge) to chromosomes prepared from a normal mouse splenic culture stimulated with lipopolysaccharide for 48 h and detected as described (18). Chromosomes were counterstained with 4,6-diamidino-2-phenylindole, and images were captured using a CCD camera and MacProbe Version 4 software (Perceptive Scientific Instruments, Inc., League City, TX).

RNA Preparation—Total RNAs from the KG1A, K562, U937, TF1, Calu-1, and KATO-III cell lines, and from human bone marrow stromal cells, and from murine strain 129 testis were extracted using the RNAzol or guanidinium isothiocyanate protocol (19, 20).

PCR Analysis of cDNAs—PCR analyses were carried out with Marathon-Ready cDNAs derived from human bone marrow, placenta, spleen, kidney, and colon or with a murine cDNA panel derived from adult mouse heart, brain, spleen, lung, liver, skeletal muscle, kidney, and testis and from day 7, 11, 15, and 17 mouse embryos (CLONTECH)

granulocyte/macrophage colony-stimulating factor; IL, interleukin; G-CSF, granulocyte colony-stimulating factor; mIg, murine Ig; PAC, P1 artificial chromosome; RT-PCR, reverse transcription-polymerase chain reaction; contig, group of overlapping clones; GAPDH, glyceraldehyde-3-phosphate dehydrogenase; UTR, untranslated region; 3′-RACE, 3′-rapid amplification of cDNA ends; kb, kilobase pair(s); bp, base pair(s); BFU-E, erythroid burst-forming unit(s); GM-CFC, granulocte/macrophage colony-forming cells.

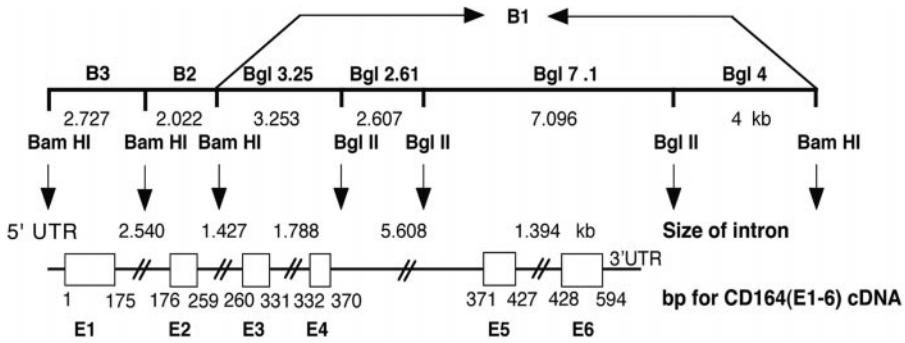

FIG. 1. **Genomic structure of human *CD164*.** Shown is a map of the intron/exon structure of the human *CD164* gene. The relationship between the genomic sequence (GenBank™/EBI accession number AF299340) and the predicted full-length human *CD164(E1–6)* nucleotide sequence (accession number AF299341) is shown. Human *CD164* cDNA probes used to screen PACs and Southern blots were prepared as follows. The *Sac*I/*Spe*I probe h1 fragment contained bp 1–1907 of cDNA sequence (where bp 1 indicates the translational start site), encompassing the whole coding sequence plus part of the 3′-UTR and part of the pRUF.*neo* vector. The *Spe*I/*Apa*I probe h2 fragment encompassed bp 1908 to 2872 of the 3′-UTR and part of the pRUF.*neo* vector. Probe h3 comprised a 1.173-kb *Eco*RV/*Hin*dIII CD164 probe from the 105A5 cDNA spanning bp 1309–2487 of untranslated *CD164* cDNA sequence in the 3′-UTR. Probe h4 comprised a 612-bp *Bst*XI/*Nco*I probe derived from bp 42 to 653 of the cDNA.

and with appropriate CD164, β-actin, or GAPDH forward and reverse primers (see Table I) using the Expand High Fidelity PCR system (Roche Molecular Biochemicals) as described by the manufacturer. The products were subcloned into the pMOS-Blue T vector (Amersham Pharmacia Biotech) and sequenced.

RT-PCR Analysis of RNA—Total human RNAs (2 μg) were reversed-transcribed by standard techniques. PCRs were then carried out as described above on these transcribed cDNAs using CD164 reverse oligonucleotide primers RD1–RD6, MGC-24-B7, MGC-GP-B2, and MGC-GP-B5 (within exons 1–6 and in the 3′-UTR) and the F164 forward primer at the translational start site and GAPDH positive control primers (GAPDH-F and GAPDH-R) (see Table I). The PCR products were subcloned into the pMOS-Blue T vector and automatically sequenced using a 3 pM concentration of the appropriate forward or reverse primer.

3′-Rapid Amplification of cDNA Ends (3′-RACE)—The 3′-ends of the human and murine *CD164* mRNAs were determined by 3′-RACE using Marathon-Ready cDNAs derived from human bone marrow, placenta, spleen, kidney, and colon or from murine testis as templates. The reaction mixtures contained 200 ng of each cDNA sample and a 10 μM concentration of either primer MGC-GP-F2 or MGC-GP-F4 for human or primer mCD164-E5F, mCD164-E6F1, mCD164–3F8, or mCD164–3F10 for mouse and reverse adaptor primer 1 or 2 (see Table I) together with 200 μM each dNTP (Amersham Pharmacia Biotech), *Taq*/PWO (*Pyrococcus woesi*) DNA polymerase mixture (Expand Long Template PCR system), and *Taq* antibody (CLONTECH) in Expand Long buffer using the Expand Long Template PCR system according to the manufacturer's instructions and standard conditions. The PCR products were subcloned into the pMOS-Blue T or pGEM T-easy vector prior to automatic sequencing using the appropriate forward or reverse primers.

Northern Blot Analysis—Human multiple hematopoietic and non-hematopoietic tissue Northern blots containing poly(A)$^+$ mRNAs were purchased from CLONTECH. The blots were probed with α-^{32}P-labeled probes CD164(E1), CD164(E1–4), CD164(E4), CD164(E5), CD164(E6), CD164-PolyA-2, CD164-PolyA-3, and GAPDH, which were generated by PCR amplification as detailed above from the human bone marrow-derived *CD164(E1–6)* cDNA with the respective primer pairs (see Table I and Fig. 3*A*): F164 and RD1, F164 and RD4, EXON4-F and RD4, EXON5-F and RD5, CD164(E6)-TM-F and MGC-24-B7, MGC-GP-F4 and MGC-GP-B4, MGC-F7 and CD164-PolyA-3, and GAPDH-F and GAPDH-R. Probes were labeled with [α-^{32}P]dCTP using the sequence-tagged site method (21). The human β-actin (CLONTECH) or GAPDH probe was labeled with [α-^{32}P]dCTP using the Megaprime kit. A murine multiple tissue Northern blot containing poly(A)$^+$ mRNAs from murine heart, brain, lung, liver, skeletal muscle, kidney, and testis was probed with [α^{32}-P]dCTP-labeled murine CD164 probe m1 (described in the legend to Fig. 6*A*). Murine strain 129 testis total RNA was Northern-blotted onto Hybond N membranes (Amersham Pharmacia Biotech) using standard techniques. Using GAPDH (see Table I) and β-actin probes, similar mRNA levels were found in the different tissues (data not shown), indicating essentially even loading of poly(A)$^+$ RNA in the different lanes. The blots were probed with ^{32}P-labeled murine probe m1 or m3 (see Fig. 6, *A* and *E*). The latter was generated by sequence-tagged site labeling of the PCR products from mouse *CD164* cDNA using the mCD164–3F10 and mCD164–3R6 primers (see Table I).

RNase Protection—Two human CD164 probes were constructed for the RNase protection assay. The first probe, PE1, spanning exon 1 plus 390 bases of the 5′-UTR and 83 bases of intron 1, was prepared by digesting the 2.73-kb *Bam*HI fragment of the human PAC clone (B2.73) with the restriction enzymes *Sal*I and *Sma*I prior to subcloning into the similarly digested pSPT19 vector (Roche Molecular Biochemicals). Probe PE2, containing exons 3–5, was generated by PCR amplification of the *CD164* cDNA using the primer pairs FBAM3 and RECO1 (see Table I), followed by insertion into the *Bam*HI/*Eco*RI-digested pSPT19 vector. The long GAPDH universal control probe (GAPDH-L) was produced by PCR amplification of bone marrow-derived Marathon-Ready cDNA using primer pairs GAPDH-F and GAPDH-R, whereas the short GAPDH universal control probe (GAPDH-S) was produced by PCR amplification of the bone marrow-derived Marathon-Ready cDNA using primer pairs PGF and PGR (see Table I) and inserted into the *Hin*dII/*Hin*dIII-digested pSPT18 vector. PE1, PE2, and GAPDH plasmids, digested with the *Ksp*I, *Hin*dIII, and *Eco*RI restriction enzymes, respectively, for linearization, were labeled with [α-^{32}P]GTP (50 μCi; Amersham Pharmacia Biotech) using SP6 RNA polymerase (20 units; Roche Molecular Biochemicals) and the SP6/T7 transcription kit (Roche Molecular Biochemicals) prior to DNase I (20 units) digestion. Total RNAs (30 μg) from Calu-1 and KG1A cells were mixed with the [α-^{32}P[GTP-labeled PE1 or PE2 probe or the GAPDH positive control probes (1×10^6 cpm/probe/tube) prior to digestion with ribonucleases A (160 ng/μl) and T1 (2.8 units/μl) (Roche Molecular Biochemicals) and treatment with a 2:1 mixture of 20% (w/v) SDS and 10 mg/ml proteinase K (ICN Pharmaceuticals Ltd., Hampshire, UK) and then electrophoresed on 8% (w/v) polyacrylamide gels (Sequagel, National Diagnostics, Aylesbury, UK) using standard techniques. ^{32}P-Labeled pBR322 *Msp*I-digested DNA (New England Biolabs Inc., Hertfordshire) at 10^4 cpm was loaded per marker lane. The gels were dried on a Bio-Rad Model 583 gel dryer and exposed to Kodak X-Omat film with intensifying screens at −70 °C.

Indirect Immunofluorescence and Confocal Microscopy—Calu-1 and A431 cells were grown on glass coverslips. High density suspension cultures of KG1B cells were settled onto poly-D-lysine-coated glass coverslips for 30 min to obtain a dense lawn of attached cells that could be fixed on the coverslips. All three cell types were fixed with 4% (w/v) paraformaldehyde in phosphate-buffered saline for 30 min at room temperature, incubated with 0.25% (w/v) NH_4Cl (3 × 5 min), and then blocked and permeabilized with 1% (w/v) bovine serum albumin and 0.1% (w/v) saponin in phosphate-buffered saline for 30 min. Cells were incubated for 1 h simultaneously with two of the following primary antibodies in 0.5% (w/v) bovine serum albumin and 0.025% (w/v) saponin in phosphate-buffered saline: mouse anti-human CD164 mAbs N6B6 and 103B2/9E10 (6), fluorescein isothiocyanate-conjugated mouse anti-human transferrin receptor antibody (Dakopatts, Glostrup, Denmark), rabbit anti-early endosomal antigen-1 antibody (serum 243, a gift from Michael J. Clague) (22), and rabbit antiserum to the cytoplasmic domain of Lamp-1 (a gift from Colin R. Hopkins).[2] For primary antibody pairs derived from different species, fluorescein isothiocyanate- or Texas Red-conjugated secondary antibodies to mouse and rabbit IgG ($F(ab)_2$ fragments, developed in donkey; 10 μg/ml; Jackson

[2] C. R. Hopkins, unpublished data.

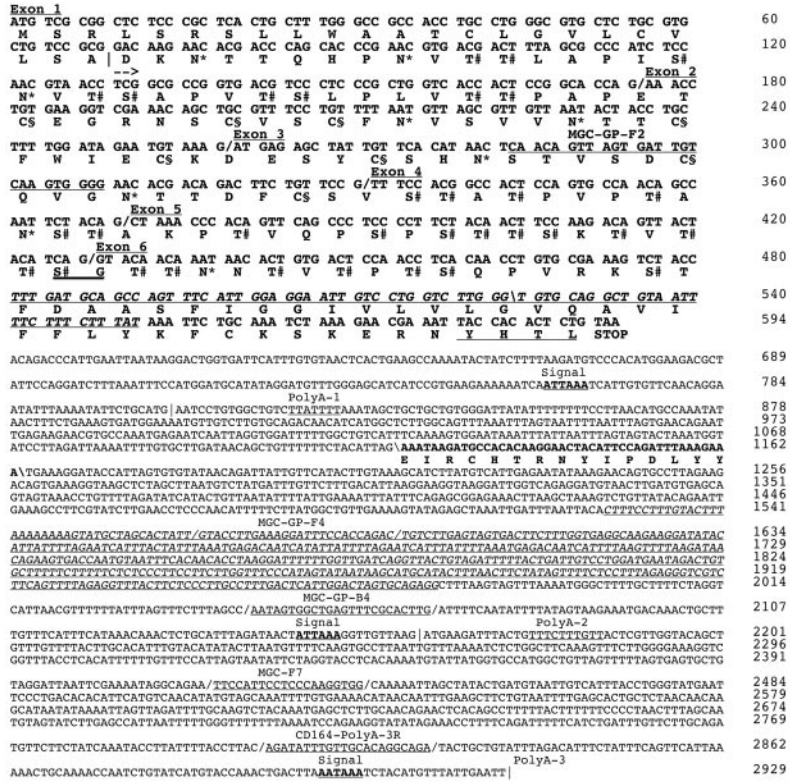

FIG. 2. **cDNA sequence of human *CD164*.** The nucleotide and predicted amino acid sequences of human *CD164(E1–6)* (GenBank™/EBI accession number AF299341) are shown. The boundaries for each exon-encoded peptide sequence are indicated (/).The signal cleavage site is marked with a *broken arrow*; the transmembrane sequence is shown in *boldface italic type* and is *underlined*; and the carboxyl-terminal YHTL amino acid motif is *boldface* and *underlined*. The presence of cysteines (§) and of predicted *N*-linked (*) and *O*-linked (#) glycosylation sites is also shown. The potential amino acids involved in the glycosaminoglycan attachment site are *double-underlined*. The positions of nucleotides used as primers (MGC-GP-F2, MGC-GP-F4, MGC-GP-B4, and MGC-F7) for 3′-RACE PCR are indicated and listed in Table I. The position of the 3′-UTR deletion that forms the *CD164(E1–6)Δ3′-UTR* splice variant is shown in *italic type* and *underlined*. The changes to the *CD164* sequence that result in the *MGC-24* sequence are marked (\). In the 3′-UTR, predicted polyadenylation sites (PolyA-1, PolyA-2, and PolyA-3) are *underlined* and labeled, whereas the signal sequence is *boldface* and *underlined*.

ImmunoResearch Laboratories, Inc., West Grove, PA) were used. When both primary antibodies were from mouse, isotype-specific fluorescein isothiocyanate- or Texas Red-conjugated secondary antibodies ($F(ab)_2$ fragments or whole IgG, developed in goat; 10 μg/ml; Southern Biotechnology Associates, Birmingham, AL) were employed. Control cells were labeled with the same two primary antibodies and only one or the other secondary antibody to ensure that no cross-reaction between isotypes was observed. Cells were mounted in Prolong Anti-fade (Molecular Probes, Leiden, The Netherlands). Confocal images were taken with a Leica TCS SP system equipped with a Leitz Plan-Apo 63× objective (NA 1.4) at a pinhole setting of 1 airy unit and a resolution of 1024 × 1024 pixels using a zoom of 2.0–4.0. Adobe Photoshop software was used for image processing.

RESULTS

Complete Sequencing of Human CD164 PAC Clones

To isolate genomic clones, a male peripheral blood leukocyte PAC library was screened with human *CD164* cDNA probes h1 and h2. Southern blotting with CD164 probe h3 demonstrated identical patterns of hybridized restriction enzyme-digested fragments from both PAC clones and from human placental genomic DNA, indicating that the PAC clones had not undergone gross rearrangements within the region of the *CD164* gene. A single hybridization band was observed with each enzyme, the largest being the *Bam*HI-restricted fragment (B1) of ~17 kb. When the blots were reprobed with cDNA probe h3, two additional *Bam*HI fragments of 2 and 3 kb (B2 and B3, respectively) were identified. These three *Bam*HI fragments span ~21 kb of DNA and contain the whole coding sequence of the human *CD164* gene (Fig. 1 and data not shown). Thus, the human *CD164* gene comprises six exons that are interspersed with five introns of varying sizes (2.540 kb (intron 1), 1.427 kb (intron 2), 1.788 kb (intron 3), 5.608 kb (intron 4), and 1.494 kb (intron 5)). All predicted splice donor and acceptor sequences matched the G(T/A)G consensus sequence (23). As described previously, this PAC clone was used to localize the human *CD164* gene to chromosome 6q21 (6).

Identification of Four Splice Variants of Human CD164

Our previous data (5) described the partial sequence of two human *CD164* cDNA clones (103B2/9E10 and 105A5) isolated from a human bone marrow stromal cDNA expression library. Complete sequencing of these two cDNA clones revealed cDNA inserts of 2873 bp linked to additional 5′- and 3′-sequences derived from the pRUF.*neo* vector. Both clones were identical except for six base pair changes, one of which occurred in the coding sequence and resulted in an amino acid change from serine to glycine at position 89 from methionine 1 of the translational start site in the 105A5 cDNA clone (Fig. 2).

Comparison with the genomic *CD164* DNA demonstrates that these human *CD164* cDNAs are encoded by exons 1–4 and 6. To identify other splice variants of *CD164*, cDNAs were amplified from a variety of cell lines and tissues by RT-PCR using the forward primer F164, upstream from and including the ATG codon of the translational start site, and the reverse exon 1–6-specific primer RD1, RD2, RD3 RD4, RD5, or RD6 or the 3′-UTR primer MGC-24-B7, MGC-GP-B2, or MGC-GP-B5 (Table I). The resultant products were Southern-blotted using exon-specific probes (Fig. 3*A*) and sequenced. For all except the latter four primers, single RT-PCR products corresponding to the appropriate exons were generated with the hematopoietic cell lines TF1, U937, KG1A, and K562; the epithelial cell lines KATO-III and Calu-l; and normal human cultured bone marrow stromal cells, normal bone marrow mononuclear cells, and placental, spleen, kidney, and colon tissues (data not shown). With the exon 6-specific and 3′-UTR reverse primers, two different sequences were obtained in most tissues and cell lines, one containing all exons (*CD164(E1–6)*) and the other lacking exon 5 (*CD164(ΔE5)*) (Figs. 2 and 3, *B* and 3*C*). In spleen, a third isoform was also found that contained all exons but exon 4 (*CD164(ΔE4)*) (Figs. 2 and 3, *B* and *C*). A fourth splice variant was generated by PCR amplification of spleen and colon cDNAs with the F164 and MGC-GP-B5 primers (Table I). This CD164

TABLE I
Oligonucleotide sequences and PCR primers
bp 1 occurs at the translational start site. Primers preceded with "m" refer to those used for murine *CD164* analysis. *NA*, not applicable.

Primer	Position on *CD164* cDNA or genomic sequence	Sequence (5′ → 3′)
MGC-GP-B1	4472 to 4448	AGAAGTCTGTCGTGTTCCCCACTTG
CD164–2KF2	2808–2826	CTTTGGGGATGCAAAACTG
B3.5-R2	6106–6124	ATTTGGGGGCAACTGTCAG
B2.5-F6	8421 to 8398	CCACTGCGTAAGTGTTTCAAGATG
B2.5-RF7	9804–9823	GCAGGATGGATGGAAGTATG
B7-F2	16572–16590	TCCCAGGTTCAAGCGATTC
B7-R3	10494 to 10476	GATGATCTGGGGAAAGATG
B3-PCR-F1	1905–1924	GCAGGAGCAAAGCAAACGAG
B2-PCR-B1	2279–2708	ACCTTCACAGGTTTCTGGGGAG
B4-FR3	NA	GGACTGTATGCTCGCTAATG
F164	1–9	GATCGATCGCGGCCGCCGCTGAGGACACGATGTCGCGG
RD1	173 to 151	ATCCCTCGAGGGTGCCGGAGTGGTGACCAGCGG
RD2	260 to 241	ATCCCTCGAGTCTTTACATTCTATCCAAAA
RD3	332 to 313	ATCCCTCGAGACGGAACAGAAGTCTGTCGT
RD4	367 to 349	ATCCCTCGAGGTAGAATTGGCTGTTGGCAC
RD5	434 to 415	ATCCCTCGAGGTTGTACCTGATGTAGTAAC
RD6	482 to 463	ATCCCTCGAGAAGGTAGACTTTCGCACAGG
MGC-24-B7	658 to 639	AGTATTTTGGCTTCAGTGAG
MGC-GP-B2	1352 to 1327	CTGCTCACATCAAGTTACATCCTCTG
MGC-GP-B5	2293 to 2268	CTTTCCCCAAGAAACTTTGAAGCCAG
EXON4-F	332–349	TTTCCACGGCCACTCCAG
EXON5-F	371–388	CTAAACCCACAGTTCAGC
CD164E6-TM-F	526–543	GTGCAGGCTGTAATTTTC
MGC-GP-F4	1566–1591	GTACCTTGAAAGGATTTCCACCAGAC
MGC-GP-B4	2069 to 2045	CAAGTGCGAAACTCAGCCACTATTG
MGC-F7	2418–2437	TTCCATTCCTCCCAAGGTGG
CD164-PolyA-3	2824 to 2803	TCTGCCTGTGCAACAAATATCT
MGC-GP-F2	284–309	
FBAM3	259–279	GATCATGGATCCGGATGAGAGCTATTGTTCACAT
RECO1	429 to 409	GATCGAATTCACCTGATGTAGTAACTGTCTT
PGF	NA	GGTCGGAGTCAACGGATTTG
PGR	NA	GCTAGAAGCTTAAAAGCAGCCCTGGT
Adaptor primer 1	NA	CCATCCTAATACGACTCACTATAGGGC
Adaptor primer 2	NA	ACTCACTATAGGGCTCGAGCGGC
GAPDH-F	NA	AAGGTGAAGGTCGGAGTC
GAPDH-R	NA	GCATTGCTGATGATCTTG
mF164	1–20	ATGTCGGGCTCCTCCCGCCG
mR164	2797 to 2780	TTCAAGAGACTAATAAAC
mCD164-SR	622 to 602	CCAGTCCACATTAATTTAACA
mCD164-F1	939–960	GTCCCCTAGAATCCTAAAGGCT
mCD164-R3	2091 to 2072	CCAGCAAGTGACAAAGAGAT
mCD164-E5F	384–401	GCCTTCCTCTCCTACACC
mCD164-E6F1	493–511	AGCTTCATTGGAGGGATCG
mCD164–3F8	1725–1745	TTCCAATGACGATACCCTGGC
mCD164–3F10	2521–2543	GCCCTGACTCTTCACCATCTTTC
mCD164–3R6	2715–2691	AACTTCTAAGTCCAGCAGTGTCTGC
mGAPDH-F	NA	TCCACCACCCTGTTGCTGTAG
mGAPDH-R	NA	GACCACAGTCCATGCCATCACT
mBAF	NA	TCGTGCGTGACATCAAAG
mBAR	NA	TGGACAGTGAGGCCAAGA

variant (Δ3′-UTR) contained the sequence derived from exons 1 to 6, but lacked 356 bp of the 3′-UTR (Fig. 2). A homologous gene, *MGC-24*, has previously been identified in the KATO-III cell line (24). The sequence for this cDNA is identical to our cDNA sequence from bp 1 to 523, but then splices onto the 3′-UTR from bp 1120 to the TGA stop codon at bp 1164–1166. This would splice within the predicted transmembrane region and create a new 3′-amino acid sequence (Fig. 2). Considerable efforts were made to identify the *MGC-24* transcript by RT-PCR using F164 and the reverse primer MGC-GP-B2 (Table I) in our tissues and cell lines, including KATO-III, but these proved unsuccessful.

Our recent studies (8) have shown that the human CD164 protein is widely expressed in both hematopoietic and non-hematopoietic tissues. To test whether the predominant splice variant of human *CD164* contained exons 4 and 5 as in *CD164(E1–6)*, total RNAs from the colonic epithelial cell line Calu-1 (Fig. 4*B*) and from the hematopoietic cell line KG1A (Fig. 4*D*) were analyzed by an RNase protection assay. The relative levels of the different transcripts were analyzed using probe PE1 to protect exon 1 and probe PE2 to protect exons 3–5 of human *CD164* (Fig. 4, *A* and *C*). The results in Fig. 4 (*B* and *D*) clearly demonstrate major protected fragments of 109 and 171 bases for exon 1 and exons 3–5, respectively. This indicates that *CD164(E1–6)* is the major isoform in these cell lines.

Northern Blot and 3′-RACE PCR Analyses Reveal Three Species of Human CD164 mRNA with Different Polyadenylation Sites

Composite poly(A)$^+$ RNA Northern blots comprising multiple hematopoietic (Fig. 5, *A* and *C*) and non-hematopoietic (Fig. 5, *B* and *D*) tissues were analyzed using exon- and 3′-UTR-specific cDNA probes (Fig. 3*A*). Similar results were obtained whether probes to exons 1–4 (Fig. 5, *A* and *B*, respectively) or to exon 1, exon 4, exon 5, or exon 6 were used (data not shown), confirming human *CD164(E1–6)* as the major isoform in the tissues and cell lines examined. All the tissues expressed at

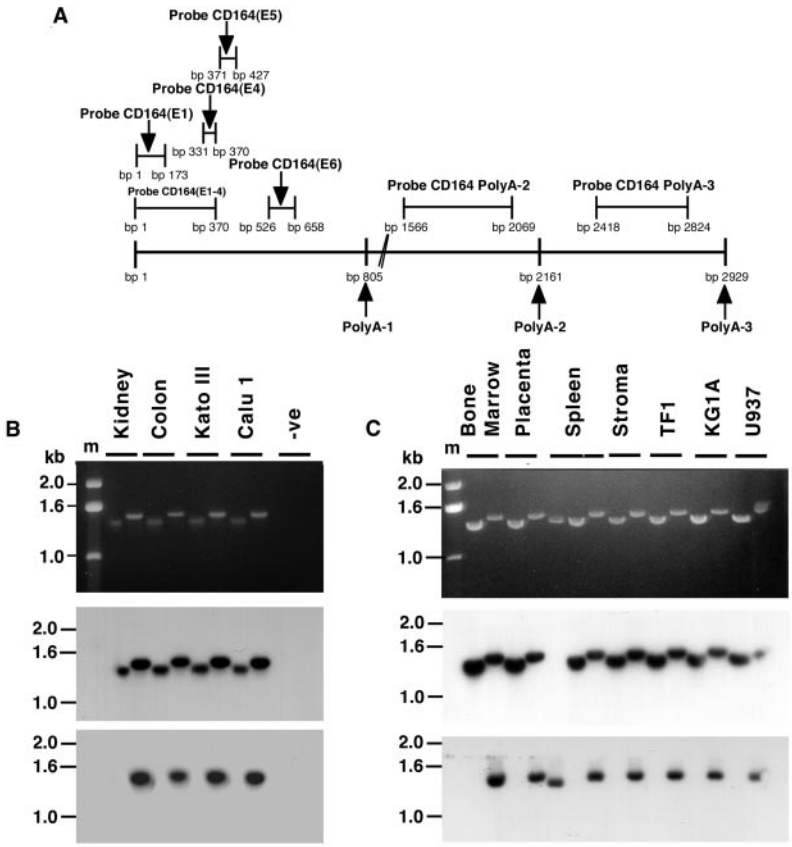

FIG. 3. **Splice variants of human *CD164* mRNAs.** *A*, shown are the exon-specific sequences derived from human *CD164(E1–6)* cDNA and used for probing Northern blots. The three polyadenylation sites (PolyA-1, PolyA-2, and PolyA-3) are labeled. *B* and *C*, RT-PCR products from human non-hematopoietic and hematopoietic tissues, respectively, and cell lines were generated using the F164 and MGC-GP-B2 primers and analyzed by agarose gel electrophoresis and ethidium bromide staining (*upper panel*) or Southern-blotted and probed using CD164(E5)-specific (*middle panel*) and CD164(E4)-specific (*lower panel*) probes. The cell lines and tissues used are indicated above the gels. *Lanes −ve* lacked DNA template. *Lanes m* contained a 1-kb DNA molecular size ladder (Life Technologies, Inc.).

least two bands of ~3.2 and 2.8 kb, except brain, which appeared to express the 3.2-kb mRNA only (Fig. 5*B*). Although the 3.2-kb band appeared to be the most prominent mRNA species in all tissues, both the 3.2- and 2.8-kb species were expressed in slightly variable amounts in the different hematopoietic tissues examined. The 2.8-kb band was more prominent in spleen, lymph node, peripheral blood leukocytes, and fetal liver, but little was detected in thymus and bone marrow (Fig. 5*A*). The variability in mRNA expression was more evident on the non-hematopoietic blot, with the most prominent bands occurring in heart and placenta (Fig. 5*B*). Moreover, some tissues expressed another band of 1.2 kb (Fig. 5*B*). This band was most obvious in placenta, but was also visible in pancreas after short autoradiographic exposures. However, after long exposures, it became evident in hematopoietic tissues and adult liver and skeletal muscle.

These Northern analyses suggested that variability in mRNA size was due to usage of different polyadenylation sites. This was confirmed by 3′-RACE PCR of cDNAs derived from bone marrow, placenta, spleen, kidney, and colon using the MGC-GP-F2 or MGC-GP-F4 forward primer (Fig. 2 and Table I) and adaptor 1 as the reverse primer (Table I). Two PCR products of ~700 and 1500 bp were generated with the MGC-GP-F4 primer, and one of 600 bp with the MGC-GP-F2 primer. Sequencing confirmed that the human *CD164* mRNAs terminated at three different polyadenylation sites, PolyA-1, PolyA-2, and PolyA-3, in human *CD164* mRNA (Fig. 2). Computer analysis of these sequences using the WebGene polyadenylation site program indicated the existence of three signal sites associated with these three polyadenylation sites (Fig. 2). The first and second signal sites (25, 26), which serve as the binding site for the 160-kDa protein cleavage polyadenylation specificity factor, are AUUAAA, and the third signal site for the cleavage polyadenylation specificity factor is AAUAAA. The U(T)-rich elements, which serve as the binding site for the 64-kDa cleavage stimulation factor protein CstF (25, 26), were also identified 10–30 bp downstream from the first and second polyadenylation sites. All three polyadenylation sites were confirmed by hybridizing Northern blots with PCR probes between PolyA-1 and PolyA-2 and between PolyA-2 and PolyA-3 (Fig. 3*A*). One band (3.2 kb) was identified with the CD164-PolyA-3 probe (Fig. 5, *C* and *D*), and two bands (3.2 and 2.8 kb) with the CD164-PolyA-2 probe; and in tissues such as placenta, all three RNA species were detected using the exon 1–4- and exon 5-specific probes (Fig. 5*B* and data not shown).

Conservation of the Genomic Structure, Chromosomal Localization, and Differential Polyadenylated mRNAs of Murine CD164

For comparison, the murine *CD164* cDNA was isolated by PCR amplification from a murine heart cDNA library and found to be essentially identical to that described for murine *MGC-24v* by Kurosawa *et al.* (13) except for two base pair changes at positions 72 and 73 from the ATG codon of the translational start site. However, these base pair changes did not alter the predicted amino acid sequence and may represent polymorphic variation between mouse strains. Sequence analysis of the murine *CD164* PAC clone 488F16 revealed an intron/exon structure identical to the human gene (Fig. 6, *A* and *B*). PCR analysis of murine adult and embryonic tissues and sequencing of the PCR products revealed that murine *CD164(E1–6)* was the major isoform detected with only one variant, *CD164(ΔE3)*, lacking exon 3, which was found in a few cases in adult heart (data not shown). Comparative analyses of murine tissue Northern blots probed with murine CD164 probe m1 (Fig. 6*A*) revealed a band at ~3.2 kb in the tissues examined, *viz.* heart, brain, lung, liver, skeletal muscle, kidney, and

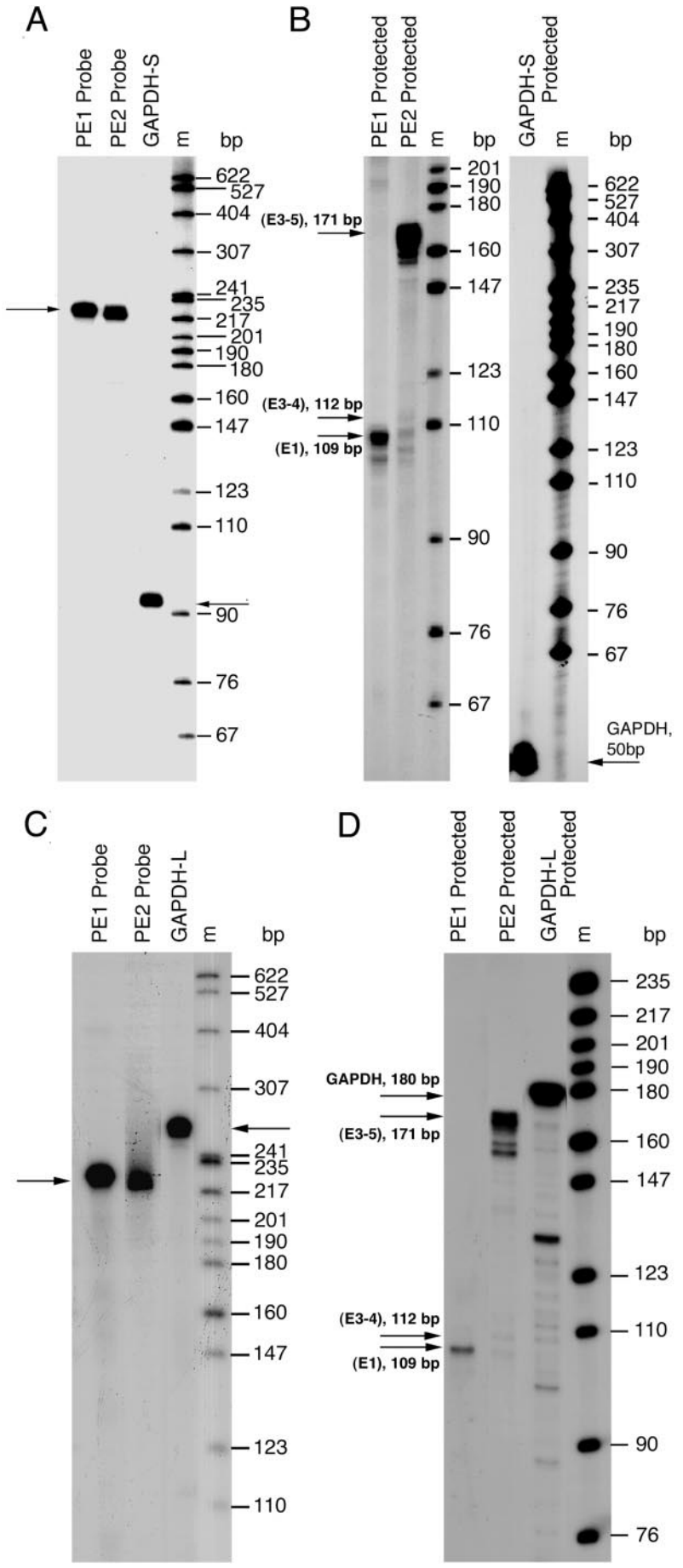

FIG. 4. **RNase protection analyses reveal that human CD164(E1–6) is the predominant isoform in Calu-1 and KG1A cells.** *A* and *C*, the ^{32}P-labeled CD164-PE1, CD164-PE2, and short and long GAPDH (GAPDH-S and GAPDH-L, respectively) control probes were hybridized with 30 μg of total RNA from the Calu-1 and KG1A cell lines, respectively, prior to treatment with RNases A and T1, and electrophoresis on 8% polyacrylamide gels. *B* and *D*, a PE1-protected RNA fragment of 109 bp, a PE2-protected RNA fragment of 171 bp, a GAPDH-S-protected RNA fragment of 50 bp, and a GAPDH-L-protected RNA fragment of 180 bp are indicated. *Lanes m* contained a ^{32}P-labeled pBR322 *Msp*I-digested DNA marker. *Arrows* indicate the positions of the unprotected probes in *A* and *C* and the protected sequences in *B* and *D*.

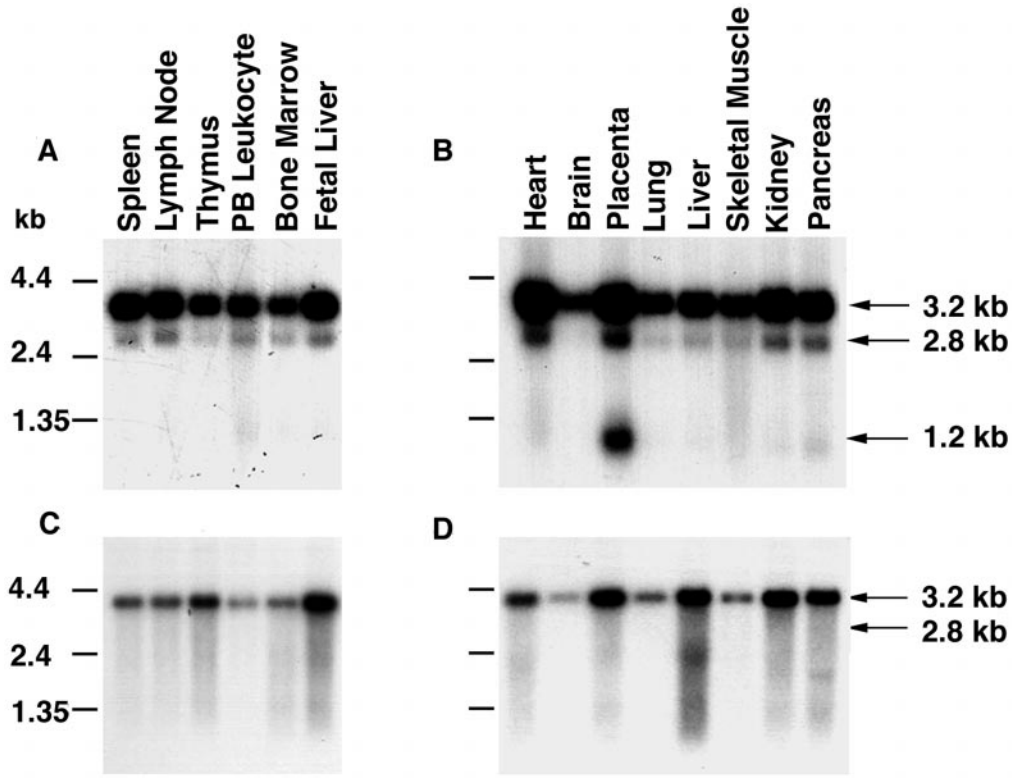

FIG. 5. **Northern blot analyses identify three *CD164* mRNA species with different polyadenylation sites.** *A* and *C*, poly(A)$^+$ RNA Northern blots from human multiple hematopoietic tissues: spleen, lymph node, thymus, peripheral blood (*PB*) leukocytes, bone marrow, and fetal liver. *B* and *D*, poly(A)$^+$ RNA Northern blots from multiple non-hematopoietic tissues: heart, brain, placenta, lung, liver, skeletal muscle, kidney, and pancreas. Blots were probed with the CD164(E1–4) (*A* and *B*) and CD164-PolyA-3 (*C* and *D*) probes indicated in Fig. 3*A*. The RNA ladder (0.24–9.5 kb) from Life Technologies, Inc. was used as the molecular size marker.

testis (Fig. 6*C*). This band was particularly prominent in liver, kidney, and testis. The 2.8-kb mRNA species was not evident on the murine Northern blot. However, it was of interest to note that in murine testis, the 1.2-kb band was also detected as a major mRNA species (Fig. 6, *C* and *D*). As with the human cDNA, 3′-RACE PCR of cDNA from murine testis and Northern blot analyses identified the 3.2- and 1.2-kb bands as RNA species with different polyadenylation sites (Fig. 6 (*D* and *E*) and data not shown). The murine PAC 488F16 clone was used to localize the murine *CD164* gene to chromosome 10B1–B2 (Fig. 7), a region syntenic with human chromosome 6q21.

Functionally Important Domains and Motifs of CD164

Protein Structure—With the intention of predicting functionally important structural features of CD164, we compared the conserved characteristics within the exon-defined amino acid sequence of human CD164(E1–6) with those of murine CD164(E1–6) and the predicted sequence of rat endolyn/CD164(E1–6) (12) (Fig. 8).

The highest amino acid identities occurred among the exon 6-encoded peptides, with 94.5 and 96.4% identities for the respective mouse and rat sequences compared with the human sequence. This high degree of homology was mainly due to the completely conserved transmembrane and cytoplasmic domains encoded by this exon. The carboxyl-terminal amino acids have been suggested to constitute a targeting motif of the type Y*XX*ø (with *X* being any amino acid and ø being a bulky hydrophobic amino acid) interacting with clathrin-adaptor complexes involved in vesicle traffic (12). Lower amino acid identities were observed for peptides encoded by exons 1 (50 and 44.8%), 2 (both 57.1%), 3 (41.7 and 37.5%), 4 (both 69.2%), and exon 5 (73.7 and 52.6%). The non-mucin domain encoded by exons 2 and 3 contains, in all these species, eight cysteines, four of which are predicted to be involved in the formation of intramolecular disulfide bridges (12). This domain links mucin domains I and II, which are encoded by exon 1 and exons 4 and 5 and part of exon 6, respectively. Using the Prosite scan protein analysis program, we confirmed the presence of sequences CFNVSVVNTTCFW, CVNATFTNNITCFW, and CVNATLTNNITCVW in the exon 2-encoded non-mucin domains of human, mouse, and rat CD164, respectively (12). These sequences belong to the consensus sequence C(LVFYR)$X_{7,8}$(STIVDN)-C*X*W, one of two cytokine receptor consensus motifs found in such molecules as the erythropoietin, G-CSF, GM-CSF, IL-4, IL-6, and thrombopoietin receptors (reviewed in Ref. 27). Both murine and human CD164(E1–6) possess 32 potential *O*-linked and 9 N-linked oligosaccharide attachment sites, whereas rat endolyn/CD164(E1–6) is predicted to contain 35 *O*-linked and 8 *N*-linked glycosylation sites. Some important characteristics of the predicted exon-defined domains of human CD164 isoforms are summarized in Table II. The similarities in the structures of human and murine CD164(E1–6) are illustrated diagrammatically in Fig. 8 (*B* and *C*).

Functional Importance of Mucin Domain I Epitopes—Our previous data indicated that CD164 is present at the surface of cells, where it may function as an adhesion molecule for attachment of CD34$^+$ hematopoietic progenitor cells to the stroma and as a negative regulator of CD34$^+$CD38$^{lo/-}$ hematopoietic progenitor cell proliferation (5). The class I and II epitopes of human CD164 defined by mAbs 105A5 and 103B2/9E10, respectively (9), mediate these functional effects. mAb 105A5 identifies a sialic acid epitope on *O*-linked oligosaccharides, whereas mAb 103B2/9E10 identifies an *N*-linked oligosaccharide-containing epitope, both on mucin domain I (9) (Fig. 8*B*). Previous single cell analyses using mAb 103B2/9E10 as an inhibitor of proliferation (5) demonstrated that this mAb inhib-

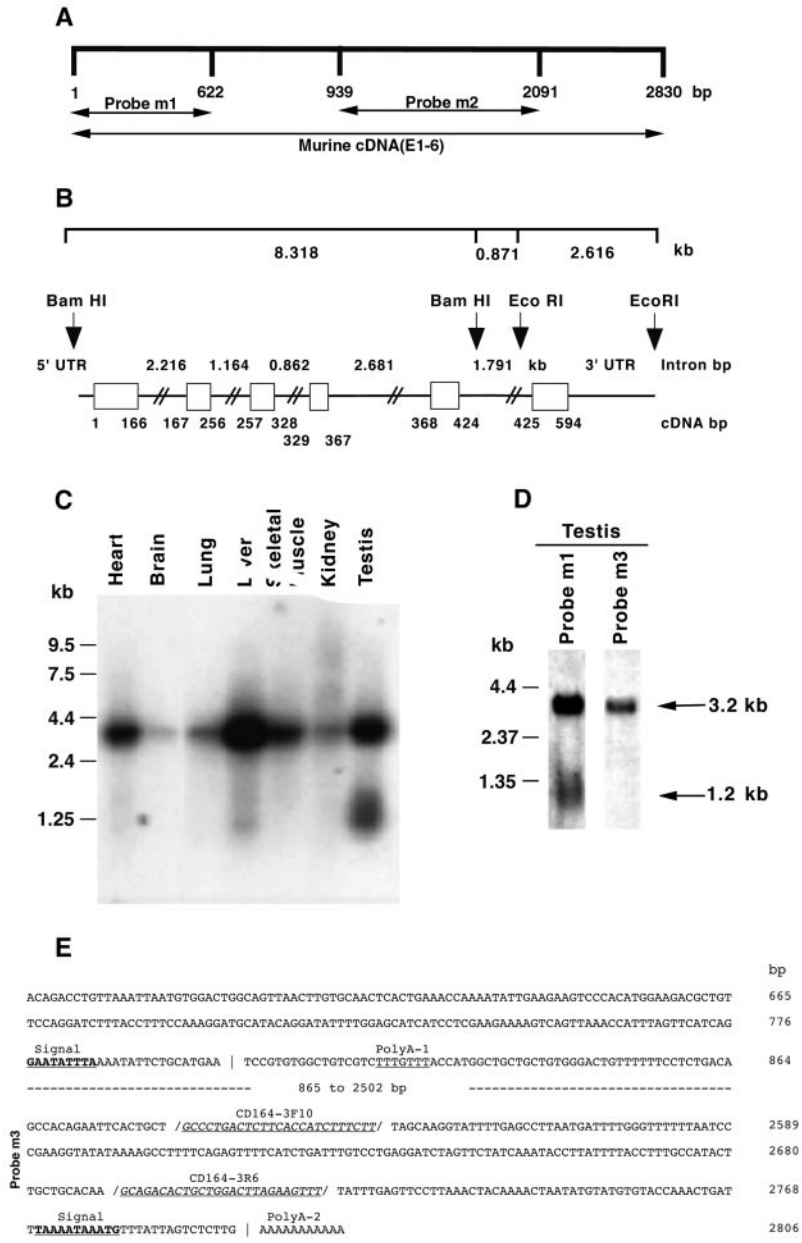

FIG. 6. **Genomic structure of murine *CD164*.** *A*, shown are the murine *CD164* cDNA probes. Murine probe m1 contained bp 1–622 of cDNA sequence, with the ATG codon at bp 1–3 as the translational start site. Probe m2 encompassed bp 939–2091 of the 3′-UTR. *B*, shown is a map of the intron/exon structure of the murine *CD164* gene. The relationship between the genomic sequence (GenBank™/EBI accession number AF299344) and the predicted full-length murine *CD164(E1–6)* nucleotide sequence (accession number AF299345) is shown. *C*, shown is a Northern blot of murine tissues containing poly(A)$^+$ mRNAs from heart, brain, lung, liver, skeletal muscle, kidney, and testis probed with probe m1. *D*, shown is a Northern blot of murine testis mRNA probed with probes m1 and m3 (see *A* and *E*). The RNA ladder (0.24–9.5 kb) from Life Technologies, Inc. was used as the molecular size marker. *E*, the potential polyadenylation sites (PolyA-1 and PolyA-2) in the 3′-UTR of murine CD164(E1–6) identified by 3′-RACE are *underlined* and labeled, and their signal sequences are in *boldface* and *underlined*. Nucleotides used to design primers mCD164–3F10 and mCD164–3R6 for PCR amplification of the murine probe m3 are shown in *italic type* and are *underlined*. *Numbers* on the right indicate the base pair position. bp 1 designates the first base pair of the predicted translational start site.

its the recruitment of single CD34$^+$CD38$^{lo/-}$ cells, the more primitive hematopoietic precursors, into the cell cycle in serum-deprived media in the presence of the cytokines IL-6, IL-3, G-CSF, and Steel factor. We have extended these experiments in Fig. 9 to further demonstrate the importance of mucin domain I. Both mAbs 105A5 and 103B2/9E10 prevented the generation of more mature nucleated cells from CD34$^+$ cells over 4 weeks of culture in serum-deprived liquid medium containing cytokines (Fig. 9*A*). That this was most likely due to inhibition of recruitment of CD34$^+$CD38$^{lo/-}$ cells into the cell cycle was further substantiated by the finding that the inhibition included nucleated cells from both the erythroid and myeloid lineages (Fig. 9, *B–E*). The growth of day 14 GM-CFC (Fig. 9, *B* and *C*) as well as BFU-E (Fig. 9, *D* and *E*) precursors from CD34$^+$ bone marrow cells was inhibited in a dose-dependent manner when clonogenic methylcellulose cultures containing cytokines were grown after preincubation of the cells with the class I and II CD164 mAbs.

Subcellular Distribution of CD164—We have demonstrated previously (6, 8) that CD164 is more highly expressed on the surface of primitive CD34$^+$CD38$^{lo/-}$ cells than on the surface of more mature CD34$^+$CD38$^+$ hematopoietic progenitor cells. Furthermore, our preliminary results indicate that, during differentiation, the majority of CD164 is lost from the cell surface and becomes distributed inside CD34$^+$CD38$^+$ cells.[3] In non-hematopoietic cells, rat endolyn/CD164(E1–6) is primarily localized in endosomal and lysosomal compartments (12, 28, 29). Thus, we examined in greater detail the intracellular localization of human CD164 in epithelium-derived cell lines (Calu-1 and A431) and in the CD34$^+$CD38$^+$ hematopoietic cell line KG1B by confocal microscopy using the class II mAb 103B2/9E10 (see above and Fig. 8*B*) or the class III mAb N6B6, which preferentially recognizes the peptide backbone encoded by exons 2 and 3 of human CD164 (Fig. 8*B*). Both antibodies generally gave a very similar labeling pattern in all three cell lines examined (data not shown). In all cases, the majority of CD164 was found in structures inside the cells (Fig. 10, *left panels*).

Cell-surface label was also observed, but, in fixed and permeabilized cells, was clearly less pronounced than the intra-

[3] S. M. Watt, unpublished data.

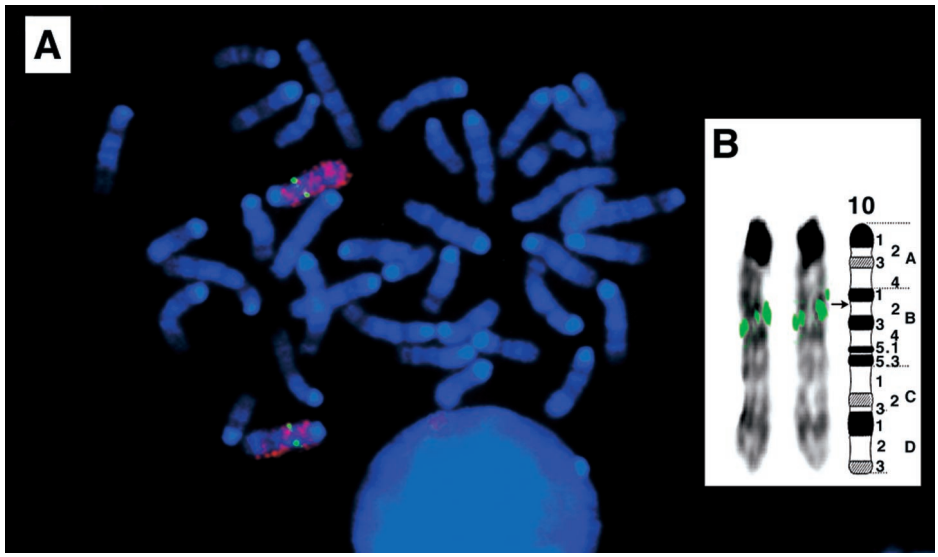

FIG. 7. **Chromosomal localization of murine *CD164*.** *A*, shown is a fluorescence *in situ* hybridization image of the PAC 488F16 signal (*arrowed*) co-localized with the mouse chromosome 10 paint on a normal mouse chromosome spread. *B*, the PAC signal (*arrowed*) is localized on mouse chromosome 10 to bands B1–B2 by comparison with a mouse chromosome 10 ideogram.

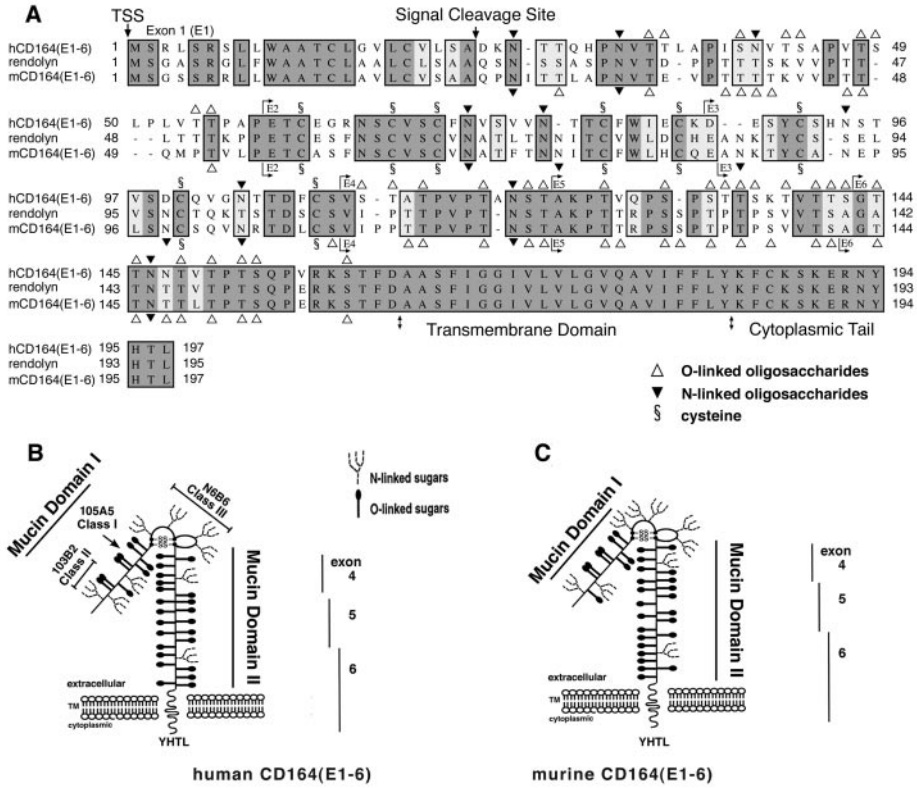

FIG. 8. **Amino acid similarities and structures of CD164 from different species.** *A*, amino acid similarities of CD164 from human, mouse, and rat determined using the ClustalW program from MacVector software. Amino acid identities (*dark gray*) and similarities (*light gray*) are indicated. The exons (E1–5), *O*-linked (△) and *N*-linked (▼) carbohydrates, and cysteine residues (§) are indicated for human CD164(E1–6) (*hCD164(E1–6)*) above the sequence and for murine CD164(E1–6) (*mCD164(E1–6)*) below the sequence. *TSS*, translational start site. The signal cleavage sites are indicated by *bent arrows*, and the transmembrane (*TM*) sequence by a *double-headed arrows*. *B* and *C*, diagrams for human and murine CD164(E1–6), respectively, highlighting mucin domains I and II; the regions defined by exons 4–6; and the positions of class I–III epitopes recognized by human CD164 mAbs 105A5, 103B2/9E10, and N6B6, respectively (9). The diagrams are based on the predicted structure of rat endolyn (*rendolyn*) (12).

cellular label. Interestingly, in agreement with previous data (8), surface CD164 was somewhat easier to detect with mAb N6B6 than with mAb 103B2/9E10. In general, the N6B6 antibody gave a slightly more homogeneous pattern with regard to the labeling intensity of CD164-positive structures within a single cell and also among cells. This was especially obvious in KG1B cells, where a minority of cells did not appear to express the 103B2/9E10 epitope or expressed it only very weakly, whereas the level of staining with mAb N6B6 was not significantly reduced. This indicated that CD164 molecules carrying the 103B2/9E10 epitope were down-regulated in a subset of KG1B cells. The common labeling pattern in all three cell lines was consistent with CD164 being primarily located in endocytic compartments. Immunoreactivity was found in punctate structures of various sizes that were located throughout the cells and that were slightly more concentrated in the perinuclear area. Antibodies to various known marker proteins for endocytic compartments were used in double labeling experiments in conjunction with mAbs N6B6 and 103B2/9E10 to confirm and to define the distribution of CD164 throughout the endocytic pathway. A good coincidence of CD164 and the lysosomal marker Lamp-1 was found in all three cell lines (Fig. 10, *E*/*F* and *I*/*K*, compare *white arrows*). In both Calu-1 and A431 cells, there were also significant numbers of strongly CD164-positive structures that were Lamp-1-negative (Fig. 10, *E* and *F*, *black arrowheads*; A431 cells not shown). These structures were identified as an early endosomal population by the presence of the marker early endosomal antigen-1 (Fig. 10, *C* and *D*), but did not appear to be recycling endosomes since they did not contain significant amounts of the transferrin receptor (data not shown). This receptor was seen in smaller punctate structures, which were enriched in two locations as expected,

TABLE II
Summary of the characteristics of predicted functional extracellular domains of human CD164

Exon-defined domains/isoforms	Classes of mAb-binding epitopes	Amino acids in mature polypeptide	*N*-Linked glycosylation sites	*O*-Linked glycosylation sites	Cysteine residues	Potential GAG[a] attachment sites
E1[b]	Class I[c]					
E1	Class II	35	3	9	0	No
E2[d]	Class III	28	2	0	5	No
E3[d]	Class III	24	2	0	3	No
E4	ND	13	1	6	0	No
E5	ND	19	0	10	0	Yes
E6	ND	55	1	7	0	No
CD164(E1–6)		197	9	32	8	Yes
CD164(ΔE4)		184	8	27	8	Yes
CD164(ΔE5)		178	9	21	8	No

[a] GAG, gycosaminoglycan; ND, not defined.
[b] After the signal sequence cleavage site. The indicated length of the exon 1-encoded peptide defines the signal sequence cleavage site between amino acids 23 and 24. Glycosylation sites were predicted with the O-glycobase and MacVector software programs. The last 45 amino acids of exon 6 comprise the transmembrane and cytoplasmic domains.
[c] The class I–III epitopes are defined by CD164 mAbs 105A5, 103B2/9E10, and N6B6, respectively.
[d] E2 and E3 together constitute a functional conformationally dependent domain.

namely, in a distinct perinuclear region and underneath or at the plasma membrane (Fig. 10*B*). Although some CD164 was also seen in small structures similar in size and number to those containing the transferrin receptor, both populations were clearly distinct from each other. In the majority of KG1B cells, CD164 was seen primarily in the same large structures as Lamp-1 (Fig. 10, *I* and *K*), although there was some overlap with early endosomal antigen-1 (data not shown). Interestingly, in a minority of KG1B cells, CD164 was found more prominently at the cell surface or in smaller vesicular structures that were positive for the transferrin receptor. This suggested that, in these cells, a significant fraction of CD164 molecules were recycling between the cell surface and early endosomes (Fig. 10, *G* and *H*). In a few of these cells, there was almost no CD164 label seen in other intracellular structures than transferrin receptor-positive endosomes, whereas other cells contained simultaneously varying amounts of label in larger structures typical of lysosomes. Altogether, these microscopy results show that, in many hematopoietic and nonhematopoietic cell lines, only a small amount of CD164 is localized at the cell surface, whereas the majority is distributed over endosomes and lysosomes. However, the variation seen among KG1B cells, *i.e.* the spectrum from almost entirely lysosomal to almost exclusively cell-surface and early and recycling endosomes, indicates that a mechanism exists by which the localization of CD164 can be regulated.

DISCUSSION

The identification of cell-surface receptors that regulate hematopoietic stem cell fate is critical to our understanding of the molecular events that control the plasticity of such cells, their proliferative capacity, their migration to the correct microenvironmental niches, and their differentiation into one of nine hematopoietic lineages. In turn, such knowledge is invaluable for clinical applications relating to stem cell usage. Recently, we have demonstrated that one such cell-surface receptor, CD164 (reviewed in Ref. 7), potentially plays a key role in regulating the recruitment of primitive $CD34^+CD38^{lo/-}$ hematopoietic stem/progenitor cells into the cell cycle (8). In this study, we have further substantiated that the two glycosylation-dependent class I and class II epitopes present on the exon 1-encoded domain are important for mediating the inhibition of $CD34^+CD38^{lo/-}$ hematopoietic progenitor cell proliferation by preventing the development of erythroid and myeloid lineages and the subsequent generation of differentiated nucleated cells *in vitro*. Both these and other recent (5, 30–33) studies indicate that CD164 as well as other hematopoietic sialomucins such as CD34, CD43, and P-selectin glycoprotein ligand-1 function as a group of negative regulators by preventing hematopoietic stem/progenitor cell proliferation and differentiation.

Moreover, in this work, we report the genomic cloning of human *CD164*. This human *CD164* gene spans at least 22 kb of DNA and contains six exons. Although all the sialomucins mentioned above have similar structural and functional characteristics, their genomic structures and chromosomal localization diverge from each other to varying degrees. For molecules such as human CD43 and P-selectin glycoprotein ligand-1, which contain mucin domains only, the cDNA coding sequence is specified by a single exon. The *CD43* and P-selectin glycoprotein ligand-1 genes encompass 4.6 and 11 kb of DNA, respectively, with each containing a single intron that interrupts the sequence specifying the 5′-untranslated region of the mRNAs. These genes are located on chromosomes 16p11.2 and 12q24, respectively (reviewed in Ref. 7). In contrast, genes such as *CD34* that contain Ig-like or non-mucin cysteine-rich domains are composed of multiple exons. The human *CD34* gene, for example, spans at least 26 kb of DNA, contains eight exons, and is situated on human chromosome 1q32. Thus, *CD164* belongs to that subgroup of mucins that are composed of multiple exons, with human *CD164* mapping to chromosome 6q21 and murine *CD164* to the syntenic chromosome 10B1–B2. This supports the view that the function of molecules such as P-selectin glycoprotein ligand-1 is regulated primarily through post-translational modifications, whereas that of molecules such as *CD164* with multiple exons may have more sophisticated regulatory mechanisms, which involve not only post-translational modifications of the oligosaccharide side chains, but also differential exon usage. The complete distribution and functional relevance of the different CD164 splice variants await further analysis.

As a prelude to generating *CD164* knockout mice for functional studies *in vivo*, we have also completely sequenced the putative mouse ortholog of human *CD164* and demonstrated a similar distribution of exons. Although differences in the intron and exon sizes are seen between the mouse and human genes, the predicted proteins are similar in size and structure. Furthermore, we have identified two and three isoforms differing in coding sequences for murine and human *CD164*, respectively. The longest isoform, *CD164(E1–6)*, which is encoded by all six exons, appears to predominate in the tissues and cell lines analyzed. This is in contrast to the originally cloned human *CD164* or *CD164(ΔE5)*, which lacks the exon 5-encoded domain. An additional transcript was detected in human

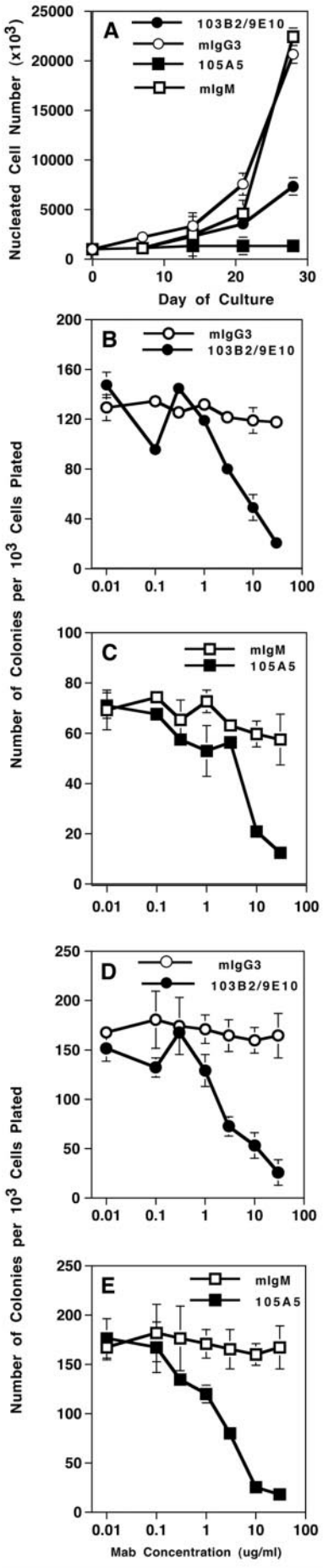

CD164 using RT-PCR amplification. This contained all six exons, but lacked 356 bp of the 3′-UTR. In agreement with the recent studies by Kurosawa *et al.* (13), the predominant mouse isoform is encoded by all six exons. A soluble isoform of human CD164 termed MGC-24 has been described previously (24). Despite extensive RT-PCR analyses, we were unable to detect this soluble variant. From analysis of our genomic sequence, this variant would be derived from exons 1 to 5 and part of exon 6, which would be spliced within the transmembrane region onto a sequence within the 3′-UTR.

On Northern blots, three human and two mouse *CD164(E1–6)* mRNAs containing different polyadenylation sites were detected, with the shortest transcript of ~1.2 kb most highly expressed in placenta and testis, respectively. The importance of these short transcripts remains to be determined. Interestingly, in a review of 33 genes, Edwalds-Gilbert *et al.* (26) identified the testis as a "hot spot" for differential polyadenylation site usage. *CD164* is an example of a gene whose expression depends on differential usage of polyadenylation sites within a single 3′-UTR. The conserved distribution of the 3.2- and 1.2-kb *CD164* transcripts between mouse and human suggests (i) that a mechanism may exist to regulate this tissue-specific polyadenylation and (ii) that differences in polyadenylation are important for the expression and function of CD164 in different tissues. Other research has suggested that genes containing multiple tandemly arrayed polyadenylation sites will select the most 5′-site preferentially. This does not seem to be the case in our studies, where the longest transcript was prevalent in all tissues. Furthermore, studies suggest that the 3′-UTR regulates both the stability and translatability of the mRNA transcript (reviewed in Refs. 34 and 35) as well as controls its nuclear export and subcellular targeting (36). In the human and murine 3.2-kb *CD164* mRNA transcripts, there are 15 and 7 AUUUA sequences, respectively. These *cis*-acting AU-rich elements are thought to be destabilizing elements in such genes as GM-CSF, c-*fos*, and interferon-β (reviewed in Refs. 26 and 36), although the optimal destabilizing sequence (UUAUUUAU) is not found in either mouse or human *CD164*. The choice of polyadenylation sites also depends on the activities and amounts of tissue-specific polyadenylation factors. Alternative polyadenylation usage, if it affects the stability and translatability of mRNA transcripts, would also affect the amount of protein transcribed and thus be of functional relevance. For example, eukaryotic initiation factor-2α contains multiple 3′-UTR polyadenylation sites. Two of the mRNA species of 1.6 and 4.2 kb that are transcribed from this gene in activated T cells show differences in stability and translatability. The 1.6-kb transcript is less stable, but more readily translated *in vitro*. Thus, an increase in polyadenylation enzyme activity as T cells move from the G_0 to S phase of the cell cycle leads to a shift to the shorter transcript and a concomitant increase in protein production (reviewed in Ref. 26). A similar

Fig. 9. **CD164 antibodies inhibit hematopoietic progenitor cell proliferation.** *A*, shown is the inhibition of nucleated cell production when CD34$^+$ cells (10^3 cells/culture) were grown in serum-deprived medium containing IL-1β, IL-3, IL-6, G-CSF, GM-CSF, and Steel factor with a 10 μg/ml concentration of CD164 mAb 103B2/9E10 or 105A5 or isotype-matched mIgG3 or mIgM mAb. Results are means ± S.E. (n = 3) of the nucleated cells generated at days 0, 14, 21, and 28 of culture. *B–E*, 561-Dynabead-purified CD34$^+$ cells (10^3 cells/culture) were incubated with 0.01–30 μg/ml concentrations of mAb 103B2/9E10 or mIgG3 (*B* and *D*) or mAb 105A5 or mIgM (*C* and *E*) for 1 h at 4 °C and then grown in methylcellulose cultures as described under "Experimental Procedures." The production of GM-CFC (*B* and *C*) and BFU-E (*D* and *E*) was scored at day 14 and is expressed as colony-forming cell frequencies. Results are means ± S.E. (n = 3) of colony numbers/10^3 cells plated.

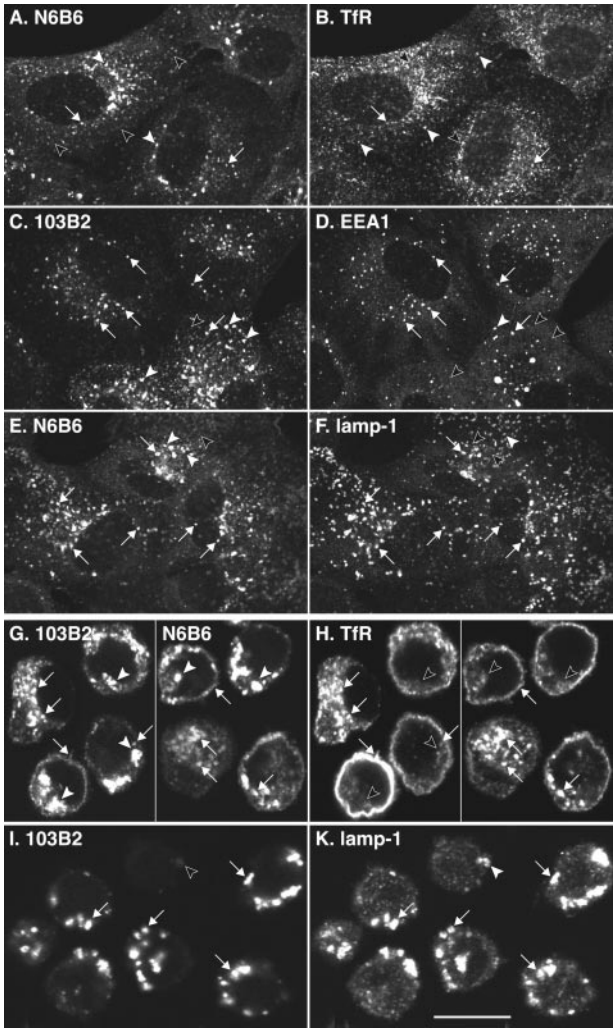

FIG. 10. **Subcellular distribution of CD164 revealed by confocal microscopy.** Calu-1 (*A–F*) and KG1B (*G–K*) cells were fixed and permeabilized and then double-labeled with one of two antibodies to CD164 (N6B6 and 103B2/9E10 as indicated (*left panels*)) and an antibody to a marker of early recycling endosomes (transferrin receptor (*TfR*); *B* and *H*), early endosomes (early endosomal antigen-1 (*EEA1*); *D*), or lysosomes (Lamp-1; *F* and *K*). *White arrows* on the corresponding *left* and *right panels* point to structures that are positive for two markers; pairs consisting of a *white* and a *black arrowhead* on the corresponding *left* and *right panels* indicate structures in which only one of the antigens is present. Note that in *A* and *B*, *white arrows* indicate the only two structures in this field in which CD164 and the transferrin receptor appear to coincide. In all other cases, the *arrows* point to just a few of many examples with overlapping label. The images in *G* and *H* are montages of four selected fields (two for each CD164 mAb shown) with cells in which CD164 is seen at the cell surface and in recycling endosomes. Cells in *I* and *K* show the average distribution of CD164 and Lamp-1 in KG1B cells. Note that one cell in the field is negative for the 103B2/9E10 epitope (*black arrowhead*). No such negative cells were seen with mAb N6B6. The *bar* represents 20 μm for *A–F* and 10 μm for *G–K*.

scenario may apply for *CD*164. However, situations in which the short transcript is up-regulated are likely to be underrepresented in the "steady-state" blots used in this study.

In addition to similarities in the long and short mRNA transcript sizes and the predominance of the *CD164(E1–6)* isoforms in both mouse and human, our studies provide further evidence to confirm that the murine gene described here is the ortholog of human *CD164*. This is evidenced by the highly conserved amino acid similarities and protein structure as a type I integral transmembrane sialomucin containing two extracellular mucin domains linked by a non-mucin domain as well as the conserved chromosomal localization. Thus, murine *CD164* provides an ideal model for the function of the human *CD164* gene *in vivo* in mouse gene knockout/knockin studies. This is particularly important if the effects of CD164 engagement by its cognate or surrogate ligands on the proliferation and adhesion of hematopoietic stem/progenitor cells *in vitro* demonstrated in this and previous (5) studies are to be reproduced *in vivo*.

Two other aspects of the structure of CD164 are of particular interest with respect to putative regulatory events. First, CD164 shares one of several conserved features of a cytokine-binding pocket (12). In this respect, it is notable that evidence exists for a class of cell-surface sialomucin modulators that directly interact with growth factor receptors to regulate their response to physiological ligands. One such example is the membrane-bound ASGP2 subunit of rat sialomucin MUC4 (37). This molecule interacts in *cis* through its epidermal growth factor-1 domain with the extracellular region of ErbB2, a cell-surface tyrosine kinase receptor implicated in embryonic cardiac and neural tissue development. ErbB2 does not appear to bind diffusible ligands directly, but instead acts as an auxiliary co-receptor to enhance signaling via the ErbB receptor network. Growth factor ligands such as neuregulin-1β bind to the related epidermal growth factor receptor to promote heterodimerization with ErbB2 and consequently to potentiate activation and signaling of the ErbB2 tyrosine kinase. Interactions of the sialomucin ASGP2 subunit with ErbB2 are thought to increase the degree of activation of ErbB receptors or the number of receptors available for activation (37). This in turn would regulate the specificity and strength of receptor signaling. In the case of CD164, the cytokine receptor motif in its non-mucin domain is reminiscent of the non-mucin ASGP2 subunit of the MUC4 sialomucin, although it is unclear if CD164 contributes to cytokine binding or signaling. However, we are now addressing this question.

Second, the cytoplasmic tail of CD164 contains a carboxyl-terminal YHTL motif of the type Y*XX*ø found in many endocytic membrane proteins or receptors (12, 38, 39). These tyrosine-based motifs bind to the μ-subunit of adaptor-protein complexes, which mediate the sorting of membrane proteins into transport vesicles from the plasma membrane to the endosomes and between intracellular compartments (38, 39). The cytoplasmic tail of rat endolyn/CD164(E1–6) has been shown to direct the targeting of the protein to endosomes and lysosomes in non-hematopoietic cells (12). Here, we have demonstrated that human CD164 is not always primarily located in late endocytic compartments. Although this was the usual distribution found in human epithelial cell lines and in the majority of KG1B cells used in this study, CD164 was more prominently expressed at the cell surface and in recycling endosomes in a minority of KG1B cells. The KG1B cell line is considered equivalent to $CD34^+CD38^+$ hematopoietic progenitor cells. Our earlier studies showed that CD164 is more highly expressed at the cell surface of primitive $CD34^+CD38^{lo/-}$ progenitor cells than on the more mature $CD34^+CD38^+$ progenitors (6, 8). The current results are consistent with the notion that a minority of KG1B cells have a more primitive phenotype. It may be that CD164 present at the cell surface binds its cognate ligand, which is internalized together with its receptor into endocytic compartments, where it is possibly released while CD164 returns via recycling endosomes back to the cell surface. The distribution of CD164 in the majority of KG1B cells indicates that, in later stages of $CD34^+$ cell maturation, the distribution of CD164 is shifted toward lysosomal compartments, where it is unlikely to bind its ligand. The mechanisms whereby sorting CD164 to different endocytic compartments at different stages of maturation of hematopoietic precursor cells is accomplished are not clear. However, a mechanism might be operating by

which the binding affinities of the Y*XX*ø motif in the cytoplasmic tail for different adaptor protein complexes can be regulated, *e.g.* by cytokine receptor interactions in *cis*. This would lead to changes in the surface and intracellular distribution of CD164. We have previously observed that the class II 103B2/9E10 epitope is more rapidly down-regulated from the cell surface than the class III N6B6 epitope (6, 8). Interestingly, a second small population of KG1B cells, presumably representing more mature cells, did not express the class II epitope at all or expressed it at very low levels. This suggests that another regulatory mechanism exists that influences the glycosylation pattern of CD164 and thus the binding characteristics regarding its ligand(s). Whether different intracellular trafficking routes are regulated by differential glycosylation of CD164 or vice versa remains to be determined. However, it is possible that both events are interconnected and contribute to the regulation of CD164 function.

In this study, we have demonstrated that human and murine CD164/endolyn are highly conserved with respect to their glycoprotein and gene structures and their chromosomal locations. Furthermore, we show that, in both species, the major isoform is encoded by all six *CD164* exons and that this maintains functionally important motifs that regulate cell proliferation or subcellular distribution. Thus, this is the first step in our aim to define the nature, expression, and regulated expression of the natural cellular ligands and binding partners for CD164. The availability in a variety of species of the genomic structures and of a defined set of *CD164* cDNAs and antibodies plus the identification of functionally important modules and motifs will permit the critical definition of CD164 functions and will aid in determining structure, function, and signaling relationships both *in vitro* and *in vivo*.

Acknowledgments—We thank Professors P. Sissons and A. C. Minson for access to the Leica confocal microscope, Dr. A. J. Thomson for advice on the RNase protection assay, Dr. K. Clark for advice on sequencing, and Dr. M. J. Clague and Professor C. R. Hopkins for providing antibodies. We also thank Professor D. J. Weatherall and Dr. J. P. Luzio for support.

REFERENCES

1. Weissman, I. L. (2000) *Cell* **100,** 157–168
2. Fuchs, E., and Segre, J. A. (2000) *Cell* **100,** 143–155
3. Verfaillie, C. M. (1998) *Blood* **92,** 2609–2612
4. Whetton, A. D., and Graham, G. J. (1999) *Trends Cell Biol.* **9,** 223–228
5. Zannettino, A. C. W., Bühring, H.-J., Niutta, S., Watt, S. M., Benton, M. A., and Simmons, P. J. (1998) *Blood* **92,** 2613–2628
6. Watt, S. M., Bühring, H.-J., Rappold, I., Chan, J. Y.-H., Lee-Prudhoe, J. E., Jones, T., Zannettino, A. C. W., Simmons, P. J., Doyonnas, R., Sheer, D., and Butler, L. H. (1998) *Blood* **92,** 849–866
7. Watt, S. M., and Chan, J. Y.-H. (2000) *Leuk. Lymphoma* **37,** 1–25
8. Watt, S. M., Butler, L. H., Tavian, M., Bühring, H.-J., Rappold, I., Simmons, P. J., Zannettino, A. C. W., Buck, D., Fuchs, A., Doyonnas, R., Chan, J. Y.-H., Levesque, J.-P., Peault, B., and Roxannis, I. (2000) *Blood* **95,** 3113–3124
9. Doyonnas, R., Chan, J. Y.-H., Butler, L. H., Rappold, I., Lee-Prudhoe, J. E., Zannettino, A. C. W., Simmons, P. J., Bühring, H.-J., Levesque, J.-P., and Watt, S. M. (2000) *J. Immunol.* **165,** 840–851
10. Almeida-Porada, G., Bühring, H.-J., Watt, S. M., Simmons, P. J., Rathke, G., Scheding, S., Kanz, L., Brugger, W., and Zanjani, E. D. (1999) *Blood* **94,** 462a (abstr.)
11. Hinds, K. A., Watt, S. M., Kirby, M. R., Sellers, S. E., Magnusson, M. K., and Dunbar, C. E. (1999) *Blood* **94,** 44a (abstr.)
12. Ihrke, G., Gray, S. R., and Luzio, J. P. (2000) *Biochem. J.* **345,** 287–296
13. Kurosawa, N., Kanemitsu, Y., Matsui, T., Shimada, K., Ishihama, H., and Muramatsu, T. (1999) *Eur. J. Biochem.* **265,** 466–472
14. Nielsen, H., Engelbrecht, J., Brunak, S., and von Heijne, G. (1997) *Protein Eng.* **10,** 1–6
15. Sonnhammer, E. L. L., von Heijne, G., and Krogh, A. (1998) in *Proceedings of the Sixth Conference on Intelligent Systems for Molecular Biology* (Glasgow, J., Littlejohn, T., Major, F., Lathrop, R., Sankoff, D., and Sensen, C., eds) pp. 175–182, AAAI Press, Menlo Park, CA
16. Milanesi, L., D'Angelo, D., and Rogozin, I. B. (2001) *Bioinformatics*, in press
17. Buckle, V. J., and Rack, K. A. (1993) in *Human Genetic Disease Analysis: A Practical Approach* (Davies, K. E., ed) 2nd Ed., pp. 59–80, IRL Press Ltd., Oxford
18. Triman, K. L., Davisson, M. T., and Roderick, T. H. (1975) *Cytogenet. Cell Genet.* **15,** 166–176
19. Puissant, C., and Houdebine, L. M. (1990) *BioTechniques* **8,** 148–149
20. Chomczynski, P., and Sacchi, N. (1987) *Anal. Biochem.* **162,** 156–159
21. Hirst, M. C., Bassett, J. H., Roche, A., and Davies, K. E. (1992) *Trends Genet.* **8,** 6–7
22. Mills, I. G., Jones, A. T., and Clague, M. J. (1998) *Curr. Biol.* **8,** 881–884
23. Mount, S. M., Burks, C., Hertz, G., Stormo, G. D., White, O., and Fields, C. (1992) *Nucleic Acids Res.* **20,** 4255–4262
24. Masuzawa, Y., Miyauchi, T., Hamanoue, M., Ando, S., Yoshida, J., Takao, S., Shimazu, H., Adachi, M., and Muramatsu, T. (1992) *J. Biochem.* (*Tokyo*) **112,** 609–615
25. Keller, W. (1997) *Cell* **81,** 829–832
26. Edwalds-Gilbert, G., Veraldi, K. L., and Milcarek, C. (1997) *Nucleic Acids Res.* **25,** 2547–2561
27. Bairoch, A., Bucher, P., and Hofmann, K. (1997) *Nucleic Acids Res.* **25,** 217–221
28. Ihrke, G., Neufeld, E. B. Meads, T., Shanks, M. R., Cassio, D., Laurent, M., Schroer, T. A., Pagano, R. E., and Hubbard, A. L. (1993) *J. Cell Biol.* **123,** 1761–1775
29. Croze, E., Ivanov, I. E., Kreibich, G., Adesnik, M., Sabatini, D. D., and Rosenfeld, M. G. (1989) *J. Cell Biol.* **108,** 1597–1613
30. Levesque, J.-P., Zannettino, A. C. W., Pudney, M., Niutta, S., Haylock, D. N., Snapp, K. R., Kansas, G. S., Berndt, M. C., and Simmons, P. J. (1999) *Immunity* **11,** 369–378
31. Bazil, V., Brandt, J. E., and Hoffman, R. (1997) *Stem Cells* **15,** 13–18
32. Bazil, V., Brandt, J., Chen, S., Roeding, M., Luens, K., Tsukamoto, A., and Hoffman, R. (1996) *Blood* **87,** 1272–1281
33. Fackler, M. J., Krause, D. S., Smith, O. M., Civin, C. I., and May, W. S. (1995) *Blood* **85,** 3040–3047
34. Miyamoto, S., Chiorini, J. A., Urcelay, E., and Safer, B. (1996) *Biochem. J.* **315,** 791–798
35. Proudfoot, N. (2000) *Trends Biochem. Sci.* **25,** 290–293
36. Conne, B., Stutz, A., and Vassalli, J.-D. (2000) *Nat. Med.* **6,** 637–641
37. Carraway, K. L., III, Rossi, E. A., Komatsu, M., Price-Schiavi, S. A., Huang, D., Guy, P. M., Carvajal, M. E., Fregien, N., Carothers Carraway, C. A. E., and Carraway, K. L. (1999) *J. Biol. Chem.* **274,** 5263–5266
38. Kirchhausen, T. (1999) *Annu. Rev. Cell Dev. Biol.* **15,** 705–732
39. Hirst, J., and Robinson, M. S. (1998) *Biochim. Biophys. Acta* **1404,** 173–193

Relationship between Novel Isoforms, Functionally Important Domains, and Subcellular Distribution of CD164/Endolyn

James Yi-Hsin Chan, Jane E. Lee-Prudhoe, Britt Jorgensen, Gudrun Ihrke, Regis Doyonnas, Andrew C. W. Zannettino, Veronica J. Buckle, Christopher J. Ward, Paul J. Simmons and Suzanne M. Watt

J. Biol. Chem. 2001, 276:2139-2152.
doi: 10.1074/jbc.M007965200 originally published online October 10, 2000
